

# Springback Property and Texture Distribution of Grained Pure Copper

Takashi Sakai, Hitoshi Omata, and Jun-Ichi Koyama

**Abstract**—To improve the material characteristics of single- and poly-crystals of pure copper, the respective relationships between crystallographic orientations and microstructures, and the bending and mechanical properties were examined. And texture distribution is also analyzed. A grain refinement procedure was performed to obtain a grained structure. Furthermore, some analytical results related to crystal direction maps, inverse pole figures, and textures were obtained from SEM-EBSD analyses. Results showed that these grained metallic materials have peculiar springback characteristics with various bending angles.

**Keywords**—Pure Copper, Grain Refinement, Environmental Materials, SEM-EBSD Analysis, Texture, Microstructure

## I. INTRODUCTION

ULTRA-FINE grain copper obtained by strong strain post addition processing has excellent material characteristics such as fatigue characteristics and sensitivity of stress-corrosion cracking. Today, the establishment of techniques for creating ultra-fine grain copper and the study of its fundamental properties have developed to a stage where definite results have been obtained [1]-[5].

Next, it is necessary to survey necessary processing characteristics to distribute the ultra-fine grain copper in the market to apply it to industrial products. To survey microscopic factors affecting springback characteristics is said to be indispensable to provide the market reliably with ultra-fine grain copper and to achieve high-precision of bending processing.

Accordingly, for this study, with a single-crystal material and a polycrystal material of pure copper being the object, strong strain post addition processing is performed by changing rolling reduction in series. The created processed material is subjected to V-shaped bending processing, and the springback amount is measured accurately. Thereafter, crystal orientation is observed on the ND (Normal Direction) plane bending section before and after the bending processing using an SEM-EBSD (Scanning Electron Microscope-Electron Backscatter Diffraction) apparatus. Then the mechanism of texture formation is clarified by strong strain post-addition processing and bending processing.

Takashi Sakai, is with the Faculty of Science and Engineering, Seikei University, Tokyo 180-8633, Japan (phone and fax: +81-422-37-3712; e-mail: sakai@st.seikei.ac.jp)

Hitoshi Omata and Jun-ichi Koyama, are with the Amada Co., LTD., Kanagawa 259-1196, JAPAN (e-mail: OMATA.A@amada.co.jp, and junkoyama@amada.co.jp)

## II. SPECIMEN AND EXPERIMENTAL METHOD

### A. Specimen preparation and observation method

In this study, to investigate the formation of a texture experimentally using strong strain post addition processing and the effect of the texture on bending processing, which is secondary processing, pure copper single-crystal material and polycrystal material are prepared as delivered materials. For the specimen shown in Fig. 1, using a wire-cut electric discharge machine, single-crystal specimen of two kinds are cut out from (a) a cylindrical pure copper single-crystal material of 50mm diameter and 70mm height: (b) a s[110] specimen with RD (Rolling Direction) being [110] direction, and (c) a s[112] specimen with RD in the [112] direction. Regarding sheet thickness  $t$ , the processed material subjected to strong strain post addition processing is cut out from an initial sheet thickness  $t_0$  to 50%-90% to be  $t=1$  mm after processing.

For comparison with the single-crystal material, specimen are cut out in the same way as the single-crystal material from (d) a 100mm×100mm block of JIS (Japanese Industrial Standards)-C1020, a commercially available pure copper polycrystal material. The specimen of the polycrystal material is defined as (e) a p-specimen. Strong metal rolling is performed at room temperature in the air using a two-stage mill, with a roll diameter of 100mm under conditions of a roll circumferential velocity 10.5mm/s and no lubrication.

Texture observation of an ND plane using an optical microscope is performed for the material obtained using the method described above to check the progress of micronization of crystal grains by strong strain post-addition processing. We also observed grain shape changes caused by bending stress loading. Using  $\text{NH}_3$  100ml +  $\text{H}_2\text{O}$  400ml solution, microscope observation is performed after electrolytic corrosion under 10V and corrosion time of 15s. Based on the obtained texture photographs, grain size  $d$  is measured using an average grain size area method according to the ASTM (American Society for Testing and Materials) standard.

Regarding the s[110] specimen and the p-specimen, to check changes in texture resulting from bending processing, the crystal orientation distribution is analyzed using an SEM-EBSD apparatus after mirror finishing by mechanical polishing. It was defined that, a tension side surface layer portion and a compression side surface layer portion of the bending portion ND plane are defined, respectively, as EBSD-1 and EBSD-2. A non-bending portion on the neutral axis, where no bending stress is loaded, is defined as EBSD-3.

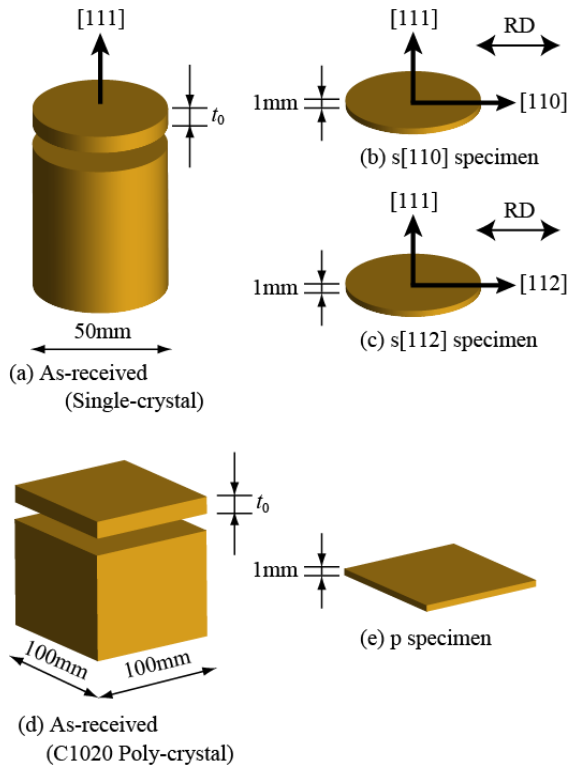


Fig. 1 Dimensions and directions of grained specimen

A bending specimen is collected using the wire-cut electric discharge machine. The shape and size of the specimen are assumed to comply with JIS-5 series specimen and the longitudinal direction is made to be parallel to RD: the bending line becomes 90 degrees against RD.

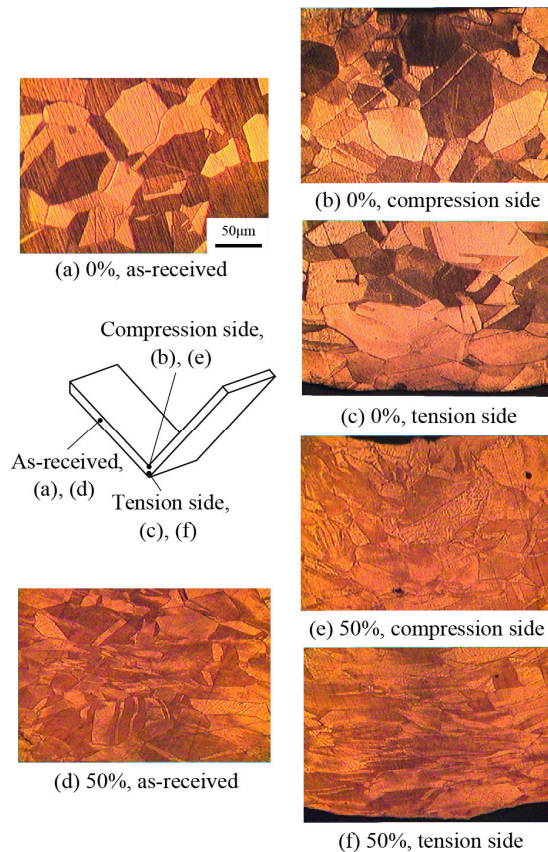
### B. Apparatus and method of bending test [6]

The bending test is performed at room temperature in air with a cross-head lowering speed being 0.5mm/min. A springback amount  $\theta_{SB}$  is measured on a real-time basis with precision of  $0.01^\circ$  ( $36''$ ), which occurs when the specimen is subjected to V-shaped folding by a die up to  $88^\circ$ ,  $90^\circ$ ,  $95^\circ$ , and  $100^\circ$  in the  $90^\circ$  direction against RD. Metal mold conditions are: punch tip  $R=0.6$ mm, punch tip angle  $88^\circ$ , V width 6mm, shoulder  $R=1.5$ mm, and die angle  $88^\circ$ .

## III. EXPERIMENT RESULTS AND CONSIDERATION

### A. Results of texture observation

Fig. 2 presents results of observing non-bending portion of the ND plane of the p-specimen and the compression side and tension side surface layer portions subjected to  $100^\circ$  bending processing as an example of texture observation. In the drawing, (a)-(c) stand for delivered materials and (d)-(f) show strong strain post-addition processed materials under rolling reduction of 50%. In (a) and (d), textures in the vicinity of the neutral axis on the ND plane with no bending stress are shown. In (a), isometric grains whose average grain size  $d=41.7\mu\text{m}$  are observed. In (d), texture is miniaturized to  $d=33.6\mu\text{m}$


 Fig. 2 Optical microscopies of p specimen for ND plane with  $100^\circ$  bending

	0%	50%	70%	90%
p specimen	○	⊙	●	●(95%)
s[110] specimen	—	△	▲	▲
s[112] specimen	□	▣	■	■

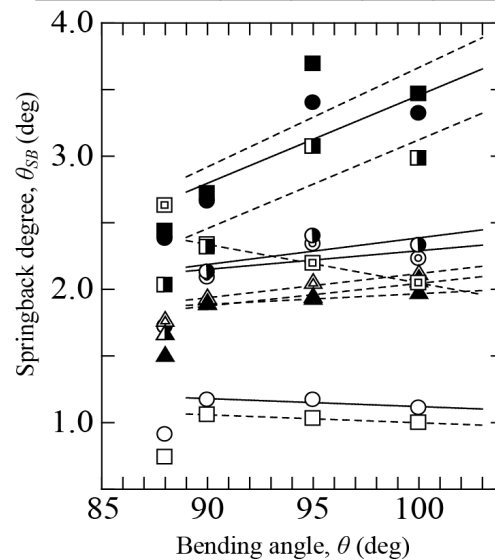
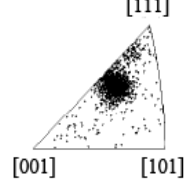
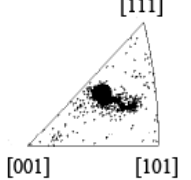
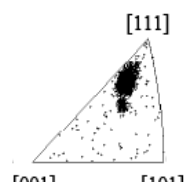
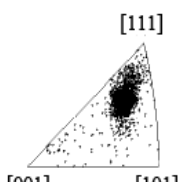
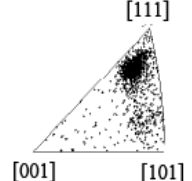
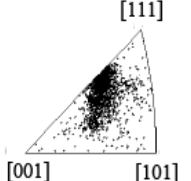
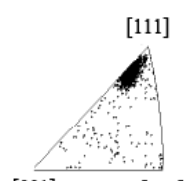
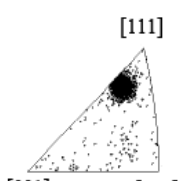

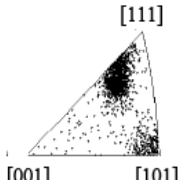
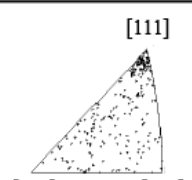
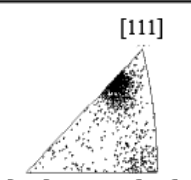


Fig. 3 Change in springback degree with bending angle.

TABLE I  
INVERSE POLE FIGURES OBTAINED BY SEM-EBSD ANALYSIS FOR S[110] SPECIMEN WITH DIFFERENT BENDING ANGLE

Compression ratio and observation area		Bending angle; 88°	Bending angle; 100°	As-received, 180°
50%	EBS-2 (Compression side)			EBS-3 (Without bending stress)
	EBS-1 (Tension side)			
70%	EBS-2 (Compression side)			EBS-3 (Without bending stress)
	EBS-1 (Tension side)			
90%	EBS-2 (Compression side)			EBS-3 (Without bending stress)
	EBS-1 (Tension side)			

caused by strong strain post addition process. In addition, miniaturization becomes such that  $d=27.5\mu\text{m}$  at rolling reduction of 70% and  $d=17.9\mu\text{m}$  at rolling reduction of 90%.

The compression and tension side surface layer portions of the bending portion of delivered materials shown in (b) and (c) of Fig. 2 remain to be isometric grains even if subjected to bending stress. However, in the 50% strong strain post addition processed materials shown in (e) and (f), crystal

grains at the tension side are expanded in the RD direction under significant influence of the bending stress; a lamellar structure is exhibited. The compression side is miniaturized while remaining isometric.

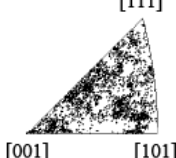
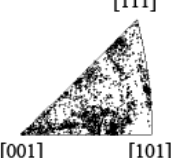
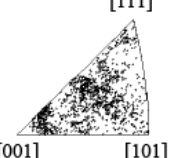
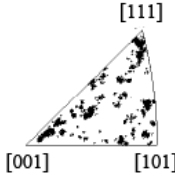
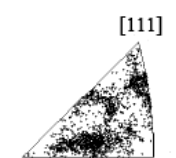
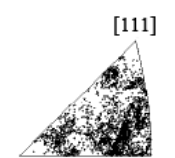


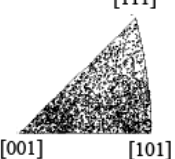
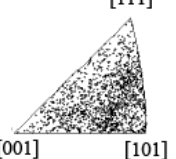
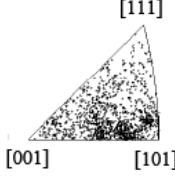
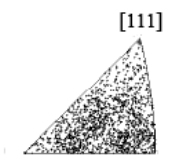
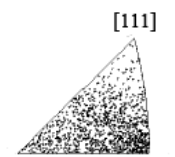
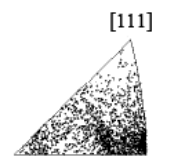
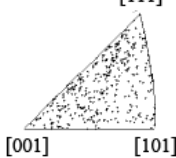
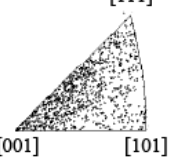
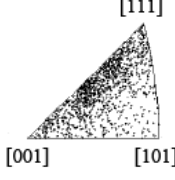
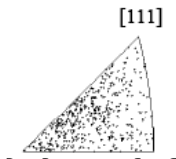

#### B. Bending test results

Fig. 3 shows changes in the spring back amount  $\theta_{\text{SB}}$  obtained using the bending test organized by each bending

angle  $\theta$ . Results show that the value of  $\theta_{SB}$  of most specimen decreases significantly as  $\theta$  changes from  $90^\circ$  to  $88^\circ$ . It is attributed to metal mold conditions such that the material is

satisfactorily accustomed to the die under the settled condition and spring back is suppressed. As the rolling reduction increases,  $\theta_{SB}$  becomes larger,

TABLE II  
INVERSE POLE FIGURES OBTAINED BY SEM-EBSD ANALYSIS FOR P SPECIMEN (JIS-C1020) WITH DIFFERENT BENDING ANGLE

Compression ratio and observation area		Bending angle; $88^\circ$	Bending angle; $90^\circ$	Bending angle; $100^\circ$	As-received, $180^\circ$
0%	EBSD-2 (Compression side)				EBSD-3 (Without bending stress) 
	EBSD-1 (Tension side)				
50%	EBSD-2 (Compression side)				EBSD-3 (Without bending stress) 
	EBSD-1 (Tension side)				
70%	EBSD-2 (Compression side)		—		EBSD-3 (Without bending stress) 
	EBSD-1 (Tension side)		—		

which is the overall trend of the drawing. However, results of the s[110] specimen show almost a constant  $\theta_{SB}$  exceptionally. Each specimen exhibits a constant  $\theta_{SB}$  in the interval between  $95^\circ$  to  $100^\circ$ . However, the same results were obtained in the case of an obtuse angle bending of  $100^\circ$  or more. It is well

known that  $\theta_{SB}$  depends on the work hardening exponent  $n$  value in general delivered materials. Changes in the  $n$  value obtained from the tension test exhibit a tendency by which the  $n$  value decreases gradually as the rolling reduction changes. Therefore, it is readily apparent that a stronger influence of

texture is imposed on  $\theta_{SB}$  obtained here than the  $n$  value. That fact suggests that when strong texture is formed at the stage of creating materials such as fine-grained materials [7]. Its plastic forming characteristics cannot be evaluated solely using conventional macroscopic mechanical properties such as the elastic modulus  $E$  and  $n$ .

### C. Changes in crystal orientation accompanied by bending processing

Table I shows a crystal orientation distribution represented by IPF (Inverse Pole Figure) with respect to changes in the rolling reduction of s[110] specimen and crystal orientation at the time of the bending processing up to  $88^\circ$  when investigating changes in crystal orientation by strong strain post addition processing and bending processing, which is secondary processing. In the table,  $180^\circ$  denotes results of the ND plane non-bending portion (EBSD-3) after strong strain post addition processing. The IPF of the EBSD-1 and EBSD-2 is also shown when the specimen is subjected to continuous bending processing up to  $100^\circ$  to  $88^\circ$ . In strong strain post-addition processing with rolling reduction of 50% or more, accumulation of 97% to [112] is observed, and a remarkable copper texture is exhibited. Application of bending stress thereafter caused a transition to [111], which is a final stable orientation of f.c.c. metal. The stress subjected to the bending portion is small so that crystal rotation is unaffected so much at the time of the  $100^\circ$  bending. Therefore, EBSD-1 and EBSD-2 exhibit different crystal orientation distributions from each other. When bent at a sharp angle up to  $88^\circ$ , sufficient bending stress is imposed at EBSD-1 and EBSD-2 respectively, resulting in a matched orientation distribution to [111], which is a final stable orientation. In EBSD-3 of 90%, [101] appears as a copper texture. When bent at  $100^\circ$ , the material exhibits the same distribution conditions as EBSD-3. However, in the case of  $88^\circ$ , that disappears and the whole material transits to [111]. Based on the facts presented above, regarding a material in which texture is formed by strong strain post-addition processing, transition stress to form different texture formation by secondary bending stress load probably exists in the stress level between  $100^\circ$ -bending and  $88^\circ$ -bending.

To compare the IPF of the s[110] specimen shown in Table 1, results obtained for the p-specimen are presented in Table 2. At EBSD-3 of the delivered material (0%), random orientation is exhibited because of annealing. In the case in which it is subjected to continuous bending processing up to  $88^\circ$ , both EBSD-1 and EBSD-2 retain random orientation. As bending stress progresses from EBSD-3, crystal rotation occurs both in the s[110] specimen and p-specimen under rolling reduction of

50% or more, causing distribution conditions to change. However, no change in orientation distribution occurs in the delivered material of the p-specimen with bending stress. Consequently, results show that considerable stress is necessary for forming texture from random orientation; no crystal rotation occurs even if bending stress is loaded. However, results show that once a texture is formed by strong strain post-addition processing, crystal orientation rotation can be generated easily even by small bending stress. That explains the difference of the springback amount in the bending test between the delivered material and the strong strain post addition processing material presented in Fig. 3. Crystal rotation occurs in the strong strain post addition processing material easily by bending processing to transit to the final stable orientation. Therefore,  $\theta_{SB}$  is apparently large because texture capable of performing elastic recovery easily is formed sequentially.

Gradual integration to [101] and [112] is observed at EBSD-3 subjected to the strong strain post addition processing of rolling reductions of 50% and 70% respectively. The same crystal orientation distribution is exhibited at both the EBSD-1 and EBSD-2 after the  $100^\circ$ -bending processing of these specimen. When these specimen are bent up to  $88^\circ$ , crystal rotation by the bending stress becomes dominant as in results of s[110] and dispersion occurs because of the integration described above, resulting in the random orientation.

## IV. SUMMARY

Pure copper single crystal and polycrystalline materials were used. Bending properties, especially the springback characteristics of materials as-received and fine-grained using the typical accumulative rolling processes, were investigated. The springback characteristics are discussed based on the texture obtained by SEM-EBSD analysis.

## REFERENCES

- [1] S. Kawahara, H. Miyamoto and T. Mimaki, *Journal of the JRICu*, Vol. 45, No. 1, 2006, pp. 190-194.
- [2] T. Nakamura and Z. Horita, *Journal of the JRICu*, Vol. 47, No. 1, 2008, pp. 98-100.
- [3] H. Miura and T. Sakai, *Journal of the JRICu*, Vol. 48, No. 1, 2009, pp. 34-38.
- [4] J. Otani, I. Sasaki, K. Hata and K. Oishi, *Journal of the JRICu*, Vol. 42, No. 1, 2003, pp. 163-167.
- [5] Y. Saito, N. Tsuji, H. Utsunomiya, T. Sakai and R. G. Hong, *Scripta Materialia*, Vol. 39, No. 9, 1998, pp. 1221-1227.
- [6] T. Sakai, K. Yoshida, J. Koyama and E. Nakamachi, *Journal of Japan Institute of Light Metals*, Vol. 59, No. 4, 2009, pp. 179-184.
- [7] T. Sakai, N. Okada, K. Yoshida J. Koyama, *Proceedings of the JSME 2006 Annual Meeting*, Vol. 1, 2006 pp. 445-446.